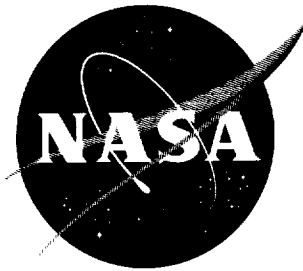


N62-15251 N62-15251

NASA TN D-1373

NASA TN D-1373



19

# TECHNICAL NOTE

D-1373

A USE OF CONFORMAL MAPPING  
TO DETERMINE THE APPARENT ADDITIONAL MASS OF  
SCALLOPED AND/OR CLUSTERED CYLINDER CONFIGURATIONS  
WITH EXPERIMENTAL EVALUATIONS OF RESULTS

By Charles E. Watkins, Donald L. Lansing,  
and Frederick W. Gibson

Langley Research Center  
Langley Station, Hampton, Va.

NATIONAL AERONAUTICS AND SPACE ADMINISTRATION  
WASHINGTON

September 1962



NATIONAL AERONAUTICS AND SPACE ADMINISTRATION

---

TECHNICAL NOTE D-1373

---

A USE OF CONFORMAL MAPPING  
TO DETERMINE THE APPARENT ADDITIONAL MASS OF  
SCALLOPED AND/OR CLUSTERED CYLINDER CONFIGURATIONS  
WITH EXPERIMENTAL EVALUATIONS OF RESULTS

By Charles E. Watkins, Donald L. Lansing,  
and Frederick W. Gibson

SUMMARY

A use is made of conformal mapping to determine equations that express the additional apparent mass of scalloped and/or clustered cylinder configurations in terms of the cross-sectional area of the configuration and the coefficients of a Fourier expansion of the logarithm of the radius vector of the configuration contour curve. Applications are made to several configurations and comparisons with experimentally determined results are made for three of the configurations considered. The calculated and experimentally determined results are found to agree satisfactorily.

INTRODUCTION

A means for calculating the stability derivatives for a given body submerged in an incompressible fluid is through a use of apparent additional masses or inertia coefficients that may be associated with the body as it undergoes various accelerated motions; see, for example, discussions on equations of motion and stability of bodies as presented in references 1 and 2. If the body under consideration is slender, certain of its stability derivatives can be closely estimated by the well-known crossflow concept of Munk (ref. 3) and Jones (ref. 4) in which case the inertia coefficients of interest are those associated with a two-dimensional potential flow about the local cross sections of the body. (See refs. 5 to 7.) Of current interest in connection with slender bodies are the inertia coefficients for sections of configurations resembling a cluster of circular cylinders, for example, the Saturn boosters, or perhaps cylindrical tanks with lengthwise corrugations that form a scalloped cross-sectional shape. These configurations will hereinafter be referred to as clustered and scalloped cylinders.

The inertia coefficients for a given configuration submerged in a perfect fluid medium can be directly related to either the kinetic energy imparted to the fluid or to the total forces that act on the configuration as it is accelerated in the fluid. This kinetic energy and/or these forces can be determined from a knowledge of the velocity potentials or, in the case of two-dimensional considerations, the complex potentials associated with the motions that the configuration undergoes. Moreover, in two-dimensional considerations the complex potentials, and hence the inertia coefficients, can be determined by means of techniques of conformal mapping which have been highly developed in connection with airfoil theory; see, for example, references 8 and 9.

Expressions of the inertia coefficients for a variety of configurations, not including clustered or scalloped cylinders, however, can be found in references 1 to 7. The purpose of this report is to make use of conformal mapping techniques to develop rather general expressions that will yield the inertia coefficients associated with translations of either clustered or scalloped cylinders. These general expressions are then applied to an elliptic cylinder (scalloped cylinder with only two lobes), for a comparison with known results, and to two special configurations for comparisons with experimentally determined results.

#### SYMBOLS

$A$	cross-sectional area
$A_n, B_n, \dots$	constants associated with transformation of velocity potential in $\zeta$ -plane (see, for example, eq. (13))
$a, b$	semiaxes of an ellipse in $\zeta$ -plane
$a_n, b_n$	constants associated with velocity potential for an arbitrary cylinder (see eq. (1))
$F_\alpha$	force per unit length acting at angle $\alpha$
$F_\xi, F_\eta$	components of force per unit length parallel to $\xi$ - and $\eta$ -axes, respectively
$g$	acceleration due to gravity
$l, L$	lengths
$M_0$	reference mass constant

$M_\alpha$	apparent additional mass per unit length associated with accelerations in direction $\alpha$
$m$	mass
$N$	number of circular cylinders involved in clustered configuration
$n$	integer
$R, R_m$	radii
$R_0, R_1, R_2, R_3$ $C$	constants
$R_m e^{i\psi(\theta)}, \theta$	polar coordinates in $\zeta$ -plane
$R_m e^{i\psi_0}, \varphi$	polar coordinates in $z$ -plane
$r$	radius vector
$t$	time
$U, u, v$	velocities
$V$	volume
$w$	complex potential
$x, y, \xi, \eta$	Cartesian coordinates
$z = x + iy$ $\zeta = \xi + i\eta$	complex variables
$\alpha$	angle measured counterclockwise from $\xi$ - and $x$ -axis
$\epsilon = \theta - \varphi$	
$\lambda, \mu, \delta$	parameters
$\lambda^n C_n, \lambda^n S_n$	Fourier coefficients
$\rho$	fluid density
$x_1, x_2$	functions of $\lambda, N, C_1, C_2$ , and so forth (see eqs. (56) and (64))

## ANALYSIS

A complex function of appropriate form is chosen to represent the complex potential associated with a cylinder of any cross-sectional shape (without circulation) and from a consideration of forces, and reactions thereto, acting on a section of this cylinder an expression for the apparent additional mass in terms of the cross-sectional area of the cylinder and certain constants appearing in the potential function is deduced.

## The Complex Potential Function and

## Apparent Additional Mass

For convenience, the origin of coordinates is chosen to be fixed at the centroid of a cross section of the cylinder and a fluid of constant density  $\rho$  is assumed to stream past the cylinder, normal to its axes, at some velocity  $U(t)$  from a direction that makes an angle  $\alpha$  with the axis of reals ( $\xi$ -axis) as indicated in figure 1. It is further assumed that the cylinder is without circulation or rotation. Under the aforementioned assumptions the complex potential,  $w(\zeta)$  will be of the form

$$w(\zeta) = -U(t) \left( \zeta e^{-i\alpha} + \frac{a_1 + ib_1}{\zeta} + \frac{a_2 + ib_2}{\zeta^2} + \dots + \frac{a_n + ib_n}{\zeta^n} + \dots \right) \quad (1)$$

where  $\zeta = \xi + i\eta$  is a complex variable,  $U(t)$  is the magnitude of the velocity at infinity and  $a_i, b_i$  are constants that depend on the cross-sectional shape of the configuration and the direction of velocity  $\alpha$ . The velocity components  $u$  and  $v$  parallel to the  $\xi$  and  $\eta$  axes, respectively, are given by the relation

$$\frac{dw}{d\zeta} = u - iv \quad (2)$$

By a use of an extended theorem of Blasius (see, for example, sections 9.52 and 9.53 of ref. 2) the components of force per unit length  $F_\xi$  and  $F_\eta$  parallel to the  $\xi$ - and  $\eta$ -axes, respectively, that act on a section of the cylinder may be expressed as

$$F_{\xi} = -\rho \frac{\partial U}{\partial t} (2\pi a_1 - A \cos \alpha) \quad (3)$$

and

$$F_{\eta} = -\rho \frac{\partial U}{\partial t} (2\pi b_1 - A \sin \alpha) \quad (4)$$

where  $A$  is the cross-sectional area of the cylinder and  $a_1$  and  $b_1$  are proportional to the real and imaginary parts, respectively, of the residue to the potential function. (See eq. (1).) The force acting on the section of the cylinder in any direction in the plane of the section can, of course, be found by appropriate projections of the components of force  $F_{\xi}$  and  $F_{\eta}$ . For example, the force  $F_{\alpha}$  acting through the centroid of the cylinder section and in the direction  $\alpha$  of the stream is

$$F_{\alpha} = F_{\xi} \cos \alpha + F_{\eta} \sin \alpha = -\rho \frac{\partial U}{\partial t} \left[ 2\pi (a_1 \cos \alpha + b_1 \sin \alpha) - A \right] \quad (5)$$

It is of interest to note that a projection of forces normal to the direction  $\alpha$  gives

$$F_{\left(\alpha + \frac{\pi}{2}\right)} = F_{\eta} \cos \alpha - F_{\xi} \sin \alpha = -2\rho\pi \frac{\partial U}{\partial t} (b_1 \cos \alpha - a_1 \sin \alpha) \quad (6)$$

As will be seen at a later stage of this analysis, this normal component of force is generally zero for clustered and/or scalloped cylinders. For cases where it is not zero, it would cause the cylinder section to rotate unless a restraining force of equal magnitude were employed.

Associated with the component of force acting in the direction  $\alpha$  on the cylinder section is a reaction in the fluid, the net total of which corresponds to an opposing force. This opposing force may be expressed as a product of time rate of change in fluid velocity and an appropriate coefficient  $M_{\alpha}$  having the dimension of a mass per unit length

$$M_{\alpha} \frac{\partial U}{\partial t} = -F_{\alpha} \quad (7)$$

This mass term  $M_\alpha$  represents the additional apparent mass or inertia coefficient of interest in the present analysis. It may be expressed in terms of  $\rho$ ,  $A$ ,  $a_1$ ,  $b_1$ ,  $U$ , and  $\alpha$  by eliminating  $F_\alpha$  between equations (5) and (7). There is obtained

$$M_\alpha = 2\pi\rho \left[ (a_1 \cos \alpha + b_1 \sin \alpha) - \frac{A}{2\pi} \right] \quad (8)$$

Equation (8) represents a key result in the present analysis. In this equation the cross-sectional area  $A$  for any given configuration can be considered as known. Thus the problem of determining  $M_\alpha$  becomes one of determining the residue  $(a_1 + ib_1)$  of the complex potential for the configuration under consideration. To this end the technique of conformal mapping developed in connection with potential theory of arbitrary wing sections (refs. 8 and 9) are readily adaptable.

#### Conformal Mapping as it Pertains to the Present Analysis

As in potential theory for two-dimensional airfoils of arbitrary shape, the basic problem in the present analysis is to determine a conformal mapping function subject to restrictions pertaining to points at infinity that will transform a cylinder of arbitrary cross-sectional shape into a circular cylinder. The inverse of this mapping function will, of course, map the region outside the determined circle into the region outside the given closed area. Furthermore, this inverse mapping function will map a potential function for the circle into a corresponding potential function for the closed area. Hence, if one determines the mapping function that will transform a cylinder of given cross-sectional shape into a circular cylinder, the coefficients  $a_n + ib_n$  (eq. (1)) can be readily obtained from the inverse transformation and the noncirculatory potential function for a circular cylinder. Details of the method of determining the appropriate mapping functions are set forth in the following section.

#### The Mapping Function and Residue of the Complex Potential for a Clustered or Scalloped Cylinder Configuration

Let a cross section of the given cylindrical configuration be assumed to be in the  $\zeta$ -plane with its boundary defined by



$$\zeta = R_m e^{\psi(\theta) + i\theta} \quad (9)$$

where  $\theta = \tan^{-1} \frac{\eta}{\xi}$  is the polar angle,  $R_m e^{\psi(\theta)} = \sqrt{\xi^2 + \eta^2}$  is the radius vector to any point on the boundary and  $\psi$  is a known function of  $\theta$ . (See fig. 1.) The constant  $R_m$  is introduced simply to preserve dimensions and for definiteness can be taken as the maximum radius of the configuration. Now let it be required to transform this configuration into a circle in the  $z$ -plane defined by

$$z = R_m e^{\psi_0 + i\varphi} \quad (10)$$

where  $\varphi$  is the polar angle and  $R_m e^{\psi_0}$  (a constant) is the radius of the circle. The general transformation for this purpose is found in the developments of references 8 and 9 to be

$$\frac{\zeta}{z} = \exp f(z) \quad (11)$$

where  $f(z)$  is an infinite series of inverse powers of  $z$ . For clustered and/or scalloped cylinder configurations it is found convenient because of symmetry, to express this series as

$$f(z) = \sum_{n=1}^{\infty} \frac{A_n + iB_n}{z^{nN}} \quad (12)$$

where  $N$  is the number of cylinders in the cluster (or corrugations on a scalloped configuration) and  $A_n$  and  $B_n$  are constants, the determination of which will be discussed along with the constant  $\psi_0$  in the following section. Note that at infinity the transformation defined by equations (11) and (12) preserves the 1:1 correspondence of  $\zeta$  and  $z$  and that  $\left| \frac{d\zeta}{dz} \right| = 1$ .

By making use of equation (12) to expand the exponential term in equation (11), the first few terms of the results may be written as

$$\zeta = z \left[ 1 + \frac{A_1 + iB_1}{z^N} + \frac{(A_2 + \frac{1}{2}C_2) + i(B_2 + D_2)}{z^{2N}} + \frac{(A_3 + C_3 + \frac{1}{6}E_3) + i(B_3 + D_3 + \frac{1}{6}F_3)}{z^{3N}} + \dots \right] \quad (13)$$

where

$$\left. \begin{aligned} C_2 &= A_1^2 - B_1^2 & E_3 &= A_1^3 - 3A_1B_1^2 \\ D_2 &= A_1B_1 & D_3 &= A_1B_2 + B_1A_2 \\ C_3 &= A_1A_2 - B_1B_2 & F_3 &= B_1^3 - 3A_1^2B_1 \end{aligned} \right\} \quad (14)$$

Inversion of equation (13) gives for the first few terms of  $z$  in terms of  $\zeta$

$$z = \zeta \left\{ 1 - \frac{A_1 + iB_1}{\zeta^N} - \frac{A_2 + \frac{2N-1}{2}C_2 + i[B_2 + (2N-1)D_2]}{\zeta^{2N}} - \frac{A_3 + (3N-1)C_3 + \frac{1}{6}(3N-1)^2E_3 + i[B_3 + (3N-1)D_3 + \frac{1}{6}(3N-1)^2F_3]}{\zeta^{3N}} + \dots \right\} \quad (15)$$

Now the complex potential for a circular cylinder of radius  $R_m e^{\psi_0}$  without circulation is

$$w(z) = -U \left( ze^{-i\alpha} + \frac{R_m^2 e^{2\psi_0} e^{i\alpha}}{z} \right) \quad (16)$$

Substituting the expression for  $z$  given in equation (15) into equation (16) and expanding gives the potential for the cylinder configuration

$$\begin{aligned}
w(\zeta) = -U \left\{ \zeta e^{-i\alpha} - \frac{A_1 + iB_1}{\zeta^{N-1}} e^{-i\alpha} - \frac{A_2 + \frac{2N-1}{2}C_2 + i[B_2 + (2N-1)D_2]}{\zeta^{2N-1}} e^{-i\alpha} \right. \\
\left. + \frac{R_m^2 e^{2\psi_0}}{\zeta} e^{i\alpha} + \frac{R_m^2 e^{2\psi_0} (A_1 + iB_1)}{\zeta^{N+1}} e^{i\alpha} + \dots \right\} \quad (17)
\end{aligned}$$

These few terms of the complex potential are enough to determine the residue  $a_1 + ib_1$ . Note the similarity of this potential function with that given in equation (1) and also note that the residue depends on the value of  $N$ ; that is,

for  $N = 1$ ,

$$\begin{aligned}
a_1 + ib_1 &= R_m^2 e^{2\psi_0} e^{i\alpha} - \left[ A_2 + \frac{C_2}{2} + i(B_2 + D_2) \right] e^{-i\alpha} \\
&= \left[ \left( R_m^2 e^{2\psi_0} - A_2 - \frac{C_2}{2} \right) \cos \alpha - (B_2 + D_2) \sin \alpha \right] \\
&\quad + i \left[ \left( R_m^2 e^{2\psi_0} + A_2 + \frac{C_2}{2} \right) \sin \alpha - (B_2 + D_2) \cos \alpha \right] \quad (18)
\end{aligned}$$

for  $N = 2$ ,

$$\begin{aligned}
a_1 + ib_1 &= R_m^2 e^{2\psi_0} e^{i\alpha} - (A_1 + iB_1) e^{-i\alpha} \\
&= \left[ \left( R_m^2 e^{2\psi_0} - A_1 \right) \cos \alpha - B_1 \sin \alpha \right] \\
&\quad + i \left[ \left( R_m^2 e^{2\psi_0} + A_1 \right) \sin \alpha - B_1 \cos \alpha \right] \quad (19)
\end{aligned}$$

for  $N > 2$ ,

$$a_1 + ib_1 = R_m^2 e^{2\psi_0} e^{i\alpha} = R_m^2 e^{2\psi_0} (\cos \alpha + i \sin \alpha) \quad (20)$$

A clustered or scalloped cylinder configuration generally implies a value of  $N$  greater than unity. Thus, substituting values of  $a_1$  and  $b_1$  obtained from equations (19) and (20) into equation (8) gives:

for  $N = 2$ ,

$$M_\alpha = 2\pi\rho \left[ \left( R_m^2 e^{2\psi_0} - \frac{A}{2\pi} \right) - A_1 \cos 2\alpha - b_1 \sin 2\alpha \right] \quad (21)$$

and for  $N > 2$ ,

$$M_\alpha = 2\pi\rho \left( R_m^2 e^{2\psi_0} - \frac{A}{2\pi} \right) \quad (22)$$

Observe that the expression for  $M_\alpha$  depends on the direction of motion  $\alpha$  when  $N = 2$ , but is independent of  $\alpha$  when  $N > 2$ . Also if the values of  $a_1$  and  $b_1$ , obtained from equation (20), are substituted into the expression for the component of force  $F_{\alpha + \frac{\pi}{2}}$  normal to the direction of

motion (eq. (6)) it is found that this component of force vanishes when  $N > 2$ .

#### Determination of $\psi_0$ , $A_1$ , and $B_1$

By substituting the expression for  $\zeta$  given in equation (9) and the expression for  $z$  given in equation (10) into the transformation given in equations (11) and (12), there is obtained

$$\exp[\psi(\theta) - \psi_0 + i(\theta - \varphi)] = \exp \left[ \sum_{n=1}^{\infty} \frac{A_n + iB_n}{\left( R_m e^{\psi_0} \right)^{nN}} (\cos nN\varphi - i \sin nN\varphi) \right] \quad (23)$$

By equating exponents on the two sides of this equation and then separating real and imaginary parts, there are obtained conjugate Fourier expressions for the differences  $\psi - \psi_0$  and  $\theta - \varphi$ , namely,

$$\psi(\theta) - \psi_0 = \sum_{n=1}^{\infty} \frac{1}{\left( R_m e^{\psi_0} \right)^{nN}} (A_n \cos nN\varphi + B_n \sin nN\varphi) \quad (24)$$

$$\theta - \varphi = \sum_{n=1}^{\infty} \frac{1}{\left(R_m e^{\psi_0}\right)^{nN}} (B_n \cos nN\varphi - A_n \sin nN\varphi) = \epsilon(\varphi) \quad (25)$$

It should be noted that through equation (25)  $\theta$  may be considered as a function of  $\varphi$  or, vice versa,  $\varphi$  may be considered as a function of  $\theta$ . It can now be recognized that  $\psi_0$  and the coefficients  $A_n$  and  $B_n$  must have the following values (see, for example, ref. 8):

$$\psi_0 = \frac{1}{2\pi} \int_0^{2\pi} \psi(\theta) d\varphi \quad (26)$$

$$A_n = \frac{\left(R_m e^{\psi_0}\right)^{nN}}{\pi} \int_0^{2\pi} \psi(\theta) \cos nN\varphi d\varphi \quad (27)$$

$$B_n = \frac{\left(R_m e^{\psi_0}\right)^{nN}}{\pi} \int_0^{2\pi} \psi(\theta) \sin nN\varphi d\varphi \quad (28)$$

It is known that two conjugate Fourier series, such as those in equations (24) and (25), are related to one another through various forms of Poisson's integral. A convenient form of this relation for the present purpose (see ref. 10) is

$$\epsilon(\varphi) = \frac{1}{2\pi} \int_0^{2\pi} \psi(\theta) \cot \frac{\varphi' - \varphi}{2} d\varphi' \quad (29)$$

This important relation, which may be looked upon as a functional equation relating  $\psi[\theta(\varphi)]$  and  $\epsilon(\varphi)$  is conducive to a rapidly converging iterative procedure for determining  $\psi[\theta(\varphi)]$ , and hence  $\psi_0$  and the coefficients  $A_n$  and  $B_n$ , from equations (26), (27), and (28).

The scheme of iteration for  $\psi[\theta(\varphi)]$  is simple in principle but involves some tedious expansions that are avoided in the examples in references 8 and 9 by recourse to graphical methods. The scheme is briefly outlined in the following paragraph and then applied to a general expression appropriate to clustered and scalloped cylinder configurations.

## The Scheme of Iteration and Results for a Cylindrical Configuration of Arbitrary Shape

It should be recalled that  $\psi$  is assumed to be initially known as a function of  $\theta$ . As a first step in the iterative process then, the conjugate to  $\psi(\theta)$  is determined by a use of equation (29) with  $\varphi$  replaced by  $\theta$ . When the conjugate to  $\psi(\theta)$  is denoted by  $\epsilon_1(\theta)$ , the next step is to form the function  $\psi(\theta + \epsilon_1)$  and determine the conjugate  $\epsilon_2$  to this function. Then  $\psi(\theta + \epsilon_2)$  is formed and its conjugate  $\epsilon_3$  is determined and so on. This process of iteration is logically termed "successive conjugates" in references 8 and 9. It is demonstrated and emphasized in these references that only a few iterations or successive conjugates are usually necessary before  $\psi(\theta + \epsilon_n)$  converges satisfactorily to  $\psi[\theta(\varphi)]$ . This is borne out in the following applications.

The logarithm of the radius vector  $R_m e^{\psi(\theta)}$  of the cross-sectional shape of any clustered or scalloped cylinder configuration can be expressed as a trigonometric series of the form

$$\log(R_m e^{\psi(\theta)}) = \log R_m + \psi(\theta) = \log R_0 + \sum_{n=1}^{\infty} \lambda^n (C_n \cos nN\theta + S_n \sin nN\theta) \quad (30a)$$

or

$$\psi(\theta) = \log\left(\frac{R_0}{R_m}\right) + \sum_{n=1}^{\infty} \lambda^n (C_n \cos nN\theta + S_n \sin nN\theta) \quad (30b)$$

where  $R_0$  is a constant of linear dimensions and  $\lambda$ ,  $C_n$ , and  $S_n$  are nondimensional constants. The constant  $\lambda$ , which may be a parameter peculiar to the configurations at hand or simply a chosen factor for the original coefficients of the trigonometric terms in the expansion of  $\psi$ , is factored out for convenience in the following developments.

In view of the following relations (see, for example, ref. 11)

$$\int_0^{2\pi} \cot \frac{\alpha - \theta}{2} d\alpha = 0 \quad (31a)$$

$$\frac{1}{2\pi} \int_0^{2\pi} \cos m\alpha \cot \frac{\alpha - \theta}{2} d\alpha = -\sin m\theta \quad (31b)$$

and

$$\frac{1}{2\pi} \int_0^{2\pi} \sin m\alpha \cot \frac{\alpha - \theta}{2} d\alpha = \cos m\theta \quad (31c)$$

the conjugate  $\epsilon_1$  to  $\psi(\theta)$  (eq. (30b)) is

$$\epsilon_1(\theta) = \sum_1^{\infty} \lambda^n (S_n \cos nN\theta - C_n \sin nN\theta) \quad (32)$$

Following the procedure discussed in the foregoing paragraphs the next step is to form the function  $\psi(\theta + \epsilon_1)$ . That is,

$$\psi(\theta + \epsilon_1) = \log\left(\frac{R_0}{R_m}\right) + \sum_{n=1}^{\infty} \lambda^n \left[ C_n \cos nN(\theta + \epsilon_1) + S_n \sin nN(\theta + \epsilon_1) \right] \quad (33)$$

In order to obtain the conjugate  $\epsilon_2$  to this expression the right-hand side may be expanded into a Taylor's series about  $\epsilon_1 = 0$  and the results rearranged in powers of  $\lambda$ . Terms of the expansion up to and including  $\lambda^2$  are

$$\begin{aligned} \psi(\theta + \epsilon_1) = & \log \frac{R_0}{R_m} + \frac{N\lambda^2}{2} (C_1^2 + S_1^2) + \lambda (C_1 \cos N\theta + S_1 \sin N\theta) \\ & + \lambda^2 \left[ \left( C_2 - \frac{N}{2} C_1^2 + \frac{N}{2} S_1^2 \right) \cos 2N\theta \right. \\ & \left. + \left( S_2 - NS_1 C_1 \right) \sin 2N\theta \right] + \dots \end{aligned} \quad (34)$$

Comparison of equation (34) with equation (24) indicates that to a first approximation  $\psi_0$ ,  $A_1$ , and  $B_1$  are as follows:

$$\psi_0 = \log \frac{R_0}{R_m} + \frac{N\lambda^2}{2} (C_1^2 + S_1^2) \quad (35a)$$

$$A_1 = \lambda \left( R_m e^{\psi_0} \right)^N C_1 \quad (35b)$$

$$B_1 = \lambda \left( R_m e^{\psi_0} \right)^N S_1 \quad (35c)$$

The expanded expression for the conjugate  $\epsilon_2$  is found from equation (34) to be

$$\begin{aligned} \epsilon_2 = & \lambda (S_1 \cos N\theta - C_1 \sin \theta) + \lambda^2 \left[ (S_2 - NS_1 C_1) \cos 2N\theta \right. \\ & \left. - \left( C_2 - \frac{N}{2} C_1^2 + \frac{N}{2} S_1^2 \right) \sin 2N\theta + \dots \right] \end{aligned} \quad (36)$$

The next step is to form the function  $\psi(\theta + \epsilon_2)$  and then expand about  $\epsilon_2 = 0$  and determine  $\epsilon_3$ , and so forth.

By extending the expansions of  $\psi(\theta + \epsilon_1)$ ,  $\psi(\theta + \epsilon_2)$ , . . . to include higher powers of  $\lambda$  and proceeding as indicated in the foregoing, all terms involving  $\lambda$  to powers up to and including the sixth are found to have converged after three iterations; that is,

$$\psi[\theta(\phi)] = \psi(\theta + \epsilon_3) + O(\lambda^7) \quad (37)$$

This relation indicates that, if  $\lambda$  is small, the process converges very rapidly. Furthermore, the converged terms of  $\psi(\theta + \epsilon_3)$  will generally be found to be sufficient for treating clustered or scalloped cylinder configurations such as would be used for missile boosters. Expressions for  $\psi_0$ ,  $A_1$ , and  $B_1$  correct to the sixth power of  $\lambda$  are found to involve at most six of the infinity of coefficients indicated in equation (33), namely,  $C_1$ ,  $C_2$ ,  $C_3$ ,  $S_1$ ,  $S_2$ , and  $S_3$ . The expressions are as follows:



$$\begin{aligned}
\psi_0 = & \log\left(\frac{R_0}{R_m}\right) + \frac{N\lambda^2}{2}(c_1^2 + s_1^2) \\
& + \frac{N\lambda^4}{8}\left[8(c_2^2 + s_2^2) + 4N(c_2c_1^2 - c_2s_1^2 + 2c_1s_1s_2) - N^2(c_1^2 + s_1^2)^2\right] \\
& + \frac{N\lambda^6}{192}\left\{288(c_3^2 + s_3^2) + 384N(c_1c_2c_3 + c_1s_2s_3 + s_1c_2s_3 - s_1s_2c_3) \right. \\
& + 48N^2\left[c_3(c_1^3 - 3c_1s_1^2) - s_3(s_1^3 - 3s_1c_1^2) - 3(c_1^2 + s_1^2)(c_2^2 + s_2^2)\right] \\
& \left. - 56N^3(c_1^2 + s_1^2)(c_1^2c_2 - s_1^2c_2 + 2c_1s_1s_2) + 11N^4(c_1^2 + s_1^2)^3\right\} \quad (38)
\end{aligned}$$

$$\begin{aligned}
A_1 = & \left(R_m e^{\psi_0}\right)^N \left\{ \lambda c_1 + \frac{N\lambda^3}{8} \left[ 12(c_1c_2 + s_1s_2) - 3Nc_1(c_1^2 + s_1^2) \right] \right. \\
& + \frac{N\lambda^5}{192} \left[ 480(c_2c_3 + s_2s_3) + 24N(9c_1^2c_3 - 9s_1^2c_3 + 18c_1s_1s_3 \right. \\
& - 2c_1c_2^2 - c_1s_2^2) - 56N^2(5c_1^3c_2 + 6c_1^2s_1s_2 + 3c_1c_2s_1^2 + 4s_1^3s_2) \\
& \left. \left. + 45N^3c_1(c_1^2 + s_1^2)^2 \right] \right\} \quad (39)
\end{aligned}$$

$$\begin{aligned}
B_1 = & \left(R_m e^{\psi_0}\right)^N \left( \lambda s_1 + \lambda^3 \left[ \frac{3N}{2}(c_1s_2 - s_1c_2) - \frac{3N^2}{8}s_1(c_1^2 + s_1^2) \right] \right. \\
& + \lambda^5 \left\{ \frac{5N}{2}(s_3c_2 - s_2c_3) + \frac{N^2}{8} \left[ 9c_1^2s_3 - 9s_1^2s_3 - 18s_1c_1c_3 \right. \right. \\
& - 2s_1c_2^2 - 2s_1s_2^2 \left. \left. - \frac{7N^3}{24} \left[ (c_1s_2 - s_1c_2)(5s_1^2 + 3c_1^2) \right. \right. \right. \right. \\
& \left. \left. \left. + c_1s_2(s_1^2 + c_1^2) \right] + \frac{15N^4}{64}s_1(c_1^2 + s_1^2)^2 \right\} \right) \quad (40)
\end{aligned}$$

Equations (38), (39), and (40) taken in conjunction with equations (21) and (22) constitute the main results of this analysis. The results are next applied to some specific configurations.

#### APPLICATIONS AND COMPARISONS WITH EXPERIMENTAL RESULTS

In order to confirm the correctness of the foregoing analysis, application of the results is first made to an elliptic cylinder for which an exact analytical expression for the apparent additional mass is known. Applications are then made to some cylinder shapes that would be of interest in connection with clustered and scalloped cylinder configurations. Some of the results of these applications are then compared with experimentally determined results.

##### Application to an Elliptical Cylinder

The cross-sectional shape of an elliptic cylinder may be expressed in Cartesian coordinates as

$$\frac{\xi^2}{a^2} + \frac{\eta^2}{b^2} = 1 \quad (a > b) \quad (41)$$

In polar coordinates  $\xi = r \cos \theta$ ,  $\eta = r \sin \theta$ , the radius vector of the ellipse is conveniently expressed as

$$r = R_m e^{\psi(\theta)} = (1 + \mu)b \frac{1}{\sqrt{1 + \mu^2 - 2\mu \cos 2\theta}} \quad (42)$$

where

$$\left. \begin{aligned} R_m &= a = \frac{1 + \mu}{1 - \mu} b \\ \mu &= \frac{a - b}{a + b} < 1 \end{aligned} \right\} \quad (43)$$

Taking the logarithm of each side of equation (42) gives

$$\begin{aligned}
\psi(\theta) &= \log \frac{(1 + \mu)b}{R_m} - \frac{1}{2} \log(1 + \mu^2 - 2\mu \cos 2\theta) \\
&= \log \frac{R_0}{R_m} + \mu \cos 2\theta + \frac{\mu^2}{2} \cos 4\theta + \dots + \frac{\mu^n}{n} \cos 2n\theta + \dots \quad (44)
\end{aligned}$$

By comparison with equation (30b) the various parameters are found to have the following values:

$$\left. \begin{aligned}
\frac{R_0}{R_m} &= (1 - \mu) \\
N &= 2 \\
\lambda &= \mu \\
C_n &= \frac{1}{n} \\
S_n &= 0
\end{aligned} \right\} \quad (45)$$

Substituting these quantities into equations (38), (39), and (40) gives:

$$\psi_0 = \log(1 - \mu) + \mu^2 + \frac{\mu^4}{2} + \frac{\mu^6}{3} \quad (46)$$

$$\left. \begin{aligned}
A_1 &= \mu \left( R_m e^{\psi_0} \right)^2 \\
B_1 &= 0
\end{aligned} \right\} \quad (47)$$

The cross-sectional area  $A$  of the cylinder is

$$A = \pi ab \quad (48)$$

Substitution of the expressions for  $\psi_0$ ,  $A_1$ , and  $A$  into equation (21) yields

$$M_{\alpha} = 2\pi\rho \left\{ b^2(1 + \mu)^2(1 - \mu \cos 2\alpha) \exp \left[ 2 \left( \mu^2 + \frac{\mu^4}{2} + \frac{\mu^6}{3} \right) \right] - \frac{ab}{2} \right\} \quad (49)$$

It may be noted that for  $\mu = 0$ , which implies that  $b = a$ , this expression reduces to

$$M_{\alpha} = \pi\rho a^2 \quad (50)$$

corresponding to the results for a circular cylinder of radius  $a$ . The exact expression for the apparent additional mass of an elliptic cylinder is (see ref. 7, page 239 for the equation for kinetic energy imparted to the fluid)

$$M_{\alpha} = \pi\rho (a^2 \sin^2 \alpha + b^2 \cos^2 \alpha) \quad (51)$$

This expression may be written in terms of  $\mu$  as

$$M_{\alpha} = 2\pi\rho \left\{ b^2(1 + \mu)^2(1 - \mu \cos 2\alpha) \exp \left[ \log \frac{1}{(1 - \mu^2)^2} \right] - \frac{ab}{2} \right\} \quad (52)$$

Since the logarithmic term in this expression can be expanded to yield

$$\log \frac{1}{(1 - \mu^2)^2} = 2 \left( \mu^2 + \frac{\mu^4}{2} + \frac{\mu^6}{3} + \dots + \frac{\mu^{2n}}{n} + \dots \right) \quad (53)$$

it may be seen that the argument of the exponential function in equation (49) is the same as the first few terms of this expansion. In fact for values of  $\mu$  less than about 0.5 (corresponding to values of eccentricity as large as 0.95), equation (49) gives essentially the same results as equation (51). In order for the procedure to apply well to cylinder shapes with higher eccentricity, or values of  $\mu$  near unity, one would need to either extend the iteration discussed in a foregoing paragraph to include terms involving  $v$  to higher powers than the sixth or to employ an intermediary transformation, as discussed for example in references 8 and 9 in connection with airfoils, that would first transform the cylinder shape into a near circle. Such an intermediary transformation is not needed with the type of cylinder configurations considered in the following paragraphs.

### Application to a Family of Scalloped Configurations

The equation of the radius vector of the periphery of the scalloped configuration considered may be expressed as

$$r = R_m e^{\psi(\theta)} = R(1 + C \cos N\theta) \quad (54)$$

where  $R$  is a dimensional constant,  $C$  is a nondimensional constant, and  $N \geq 3$ . A sketch of the configuration for  $N = 8$  is shown in figure 2. In the numerical examples that follow, the constant  $C$  is chosen so as to make the ratio of maximum radius vector to minimum radius vector a definite function of  $N$ . That is, for a given value of  $N$ ,  $C$  is determined from the relation

$$\frac{1+C}{1-C} = \frac{\left(1 + \sin \frac{\pi}{N}\right) \cos \Lambda_0}{\cos\left(\Lambda_0 - \frac{\pi}{N}\right)} \quad (55)$$

where

$$\tan \Lambda_0 = \sqrt{3} - 1 \quad (56)$$

Taking logarithms of equation (54) and expanding gives

$$\psi(\theta) = \log \frac{R}{R_m} + \log(1 + C \cos N\theta) = \log \frac{R_0}{R_m} + \sum_{n=1}^{\infty} \lambda^n C_n \cos nN\theta \quad (57)$$

where

$$\lambda = \frac{1 - \sqrt{1 - C^2}}{C} \quad (58)$$

$$C_n = \frac{2(-1)^{n+1}}{n} \quad (59)$$

and

$$\frac{R_0}{R_m} = \frac{C}{2\lambda(1 + C)} \quad (60)$$

The cross-sectional area of the configuration under consideration is found to be

$$A = \frac{1}{2} \int_0^{2\pi} r^2 d\theta = \frac{\pi R^2}{2} (2 + c^2) \quad (61)$$

By making use of equations (59) and (60) and noting in equation (57) that  $S_n = 0$ , the expression for  $\psi_0$  (eq. (38)) pertinent to the configuration can be written as

$$\psi_0 = \log \frac{c}{2\lambda(1+c)} + x_1 \quad (62)$$

where

$$x_1 = N \left[ 2\lambda^2 + \lambda^4 (1 - 2N - 2N^2) + \frac{\lambda^6}{3} (2 - 8N - 5N^2 + 14N^3 + 11N^4) \right] \quad (63)$$

The expression for  $M_\alpha$  (eq. (22)) thus becomes

$$M_\alpha = \frac{\pi \rho R^2}{2} \left[ \left( \frac{c}{\lambda} \right)^2 e^{2x_1} - (2 + c^2) \right] \quad (64)$$

It is convenient to refer the apparent additional mass of a given configuration to the apparent additional mass  $M_0$  of a circular cylinder. For this reference choose the cylinder with radius equal to the maximum radius  $R_m$  of the configuration. In the present case

$$R_m = R(1 + c) \quad (65)$$

Hence

$$M_0 = \pi \rho R^2 (1 + c)^2 \quad (66)$$

and

$$\frac{M_\alpha}{M_0} = \frac{1}{2(1+c)^2} \left[ \left( \frac{c}{\lambda} \right)^2 e^{2x_1} - (2 + c^2) \right] \quad (67)$$

This equation has been evaluated for  $N = 3, 4, \dots, 8$  and the results are shown plotted as discrete points in figure 3. As may be noted in this figure, the ratio of masses range from about 0.81 for  $N = 3$  to about 0.93 for  $N = 8$ . About the same results are obtained for this case if the terms involving  $\lambda^6$  in  $\chi_1$  (eq. (63)) are ignored. Hence these results indicate almost complete convergence of the iterative process of determining  $\psi_0$  for this case.

### Clustered Cylinder Configuration

The expression for  $\psi(\theta)$  pertaining to a cluster of  $N$  circular cylinders can be obtained from a consideration of the equation of the part of the periphery pertaining to one of the  $N$ -cylinders in the cluster. For this purpose let the polar axis of the polar coordinate system be so chosen that the angular coordinate of the cylinder centers are  $\frac{\pi}{N}, \frac{3\pi}{N}, \dots, \frac{2p-1}{N}\pi$ . (See fig. 4.) The equation of the part of the periphery pertaining to the cylinder with center at  $\theta = \frac{\pi}{N}, r = R_3$  may then be written as

$$r = R_m e^{\psi(\theta)} = R_3 \left[ \cos\left(\theta - \frac{\pi}{N}\right) + \sqrt{\cos^2\left(\theta - \frac{\pi}{N}\right) - \cos^2 \frac{\pi}{N}} \right] \quad \left(0 \leq \theta \leq \frac{2\pi}{N}\right) \quad (68)$$

Note that for this case  $R_m = R_3 \left(1 + \sin \frac{\pi}{N}\right)$ . Taking logarithms of equation (68) and expanding the results into a Fourier series in the interval  $0 \leq \theta \leq \frac{2\pi}{N}$  gives the expression for  $\psi(\theta)$  pertinent to the configuration under consideration. There is obtained

$$\psi(\theta) = \log \frac{R_3}{R_m} + C_0 + \sum_{n=1}^{\infty} C_n \cos nN\theta \quad (69)$$

where  $\lambda$  is considered to be unity and the coefficients  $C_0$  and  $C_n$  are determined as follows:

$$\begin{aligned}
C_0 &= \frac{N}{\pi} \int_0^{\frac{\pi}{N}} \log \left( \cos \theta + \sqrt{\cos^2 \theta - \cos^2 \frac{\pi}{N}} \right) d\theta \\
&= \frac{2 - N}{2} \log \left( \cos \frac{\pi}{N} \right)
\end{aligned} \tag{70}$$

(see ref. 12) and

$$\begin{aligned}
C_n &= (-1)^n \frac{2N}{\pi} \int_0^{\frac{\pi}{N}} \log \left( \cos \theta + \sqrt{\cos^2 \theta - \cos^2 \frac{\pi}{N}} \right) \cos nN\theta \, d\theta \\
&= \frac{(-1)^n}{2n} \frac{2}{\pi} \int_0^{\frac{2\pi}{N}} \frac{\cos \left( \frac{nN}{2} - \frac{1}{2} \right) \theta - \cos \left( \frac{nN}{2} + \frac{1}{2} \right) \theta}{\sqrt{2 \left( \cos \theta - \cos \frac{2\pi}{N} \right)}} d\theta \\
&= \frac{(-1)^n}{2n} \left[ P_{\frac{nN}{2}-1} \left( \cos \frac{2\pi}{N} \right) - P_{\frac{nN}{2}} \left( \cos \frac{2\pi}{N} \right) \right]
\end{aligned} \tag{71}$$

where  $P_{\frac{nN}{2}-1}$  and  $P_{\frac{nN}{2}}$  denote Legendre functions (see ref. 13).

The expression for  $\psi_0$  for the present case can be written as

$$\psi_0 = \log \left[ \frac{R_z}{R_m} \left( \sec \frac{\pi}{N} \right)^{\frac{N-2}{2}} \right] + \chi_2 \tag{72}$$

where

$$\begin{aligned}
\chi_2 &= \frac{N}{2} \left\{ C_1^2 + \frac{1}{4} \left( 8C_2^2 + 4NC_1^2C_2 - N_2C_1^4 \right) + \frac{1}{96} \left[ 288C_3^2 + 384NC_1C_2C_3 \right. \right. \\
&\quad \left. \left. + 48N^2 \left( C_1^3C_3 - 3C_1^2C_2^2 \right) - 56N^3C_1^4C_2 + 11N^4C_1^6 \right] \right\}
\end{aligned} \tag{73}$$

The cross-sectional area of the configuration under consideration is found to be



$$\begin{aligned}
A &= NR_3^2 \int_0^{\frac{\pi}{N}} \left[ \cos\left(\theta - \frac{\pi}{N}\right) + \sqrt{\left(\cos^2 - \frac{\pi}{N}\right) - \cos^2 \frac{\pi}{p}} \right]^2 d\theta \\
&= \pi R_3^2 \sin \frac{\pi}{N} \left[ \left(1 + \frac{N}{2}\right) \sin \frac{\pi}{N} + \frac{N}{\pi} \cos \frac{\pi}{N} \right] \quad (74)
\end{aligned}$$

Hence,

$$\frac{M_\alpha}{M_0} = \frac{1}{\left(1 + \sin \frac{\pi}{N}\right)^2} \left\{ \frac{2e^{2\chi_2}}{\left(\cos \frac{\pi}{N}\right)^{N-2}} - \sin \frac{\pi}{N} \left[ \left(1 + \frac{N}{2}\right) \sin \frac{\pi}{N} + \frac{N}{\pi} \cos \frac{\pi}{N} \right] \right\} \quad (75)$$

This expression has been evaluated for  $N = 3, 4, \dots, 8$  and the results are plotted as discrete points in figure 5. The ratio of apparent additional masses for this case may be noted in figure 5 to be slightly higher (ranging from about 0.86 for  $N = 3$  to about 0.96 for  $N = 8$ ) than results for the scalloped configuration in figure 3. Dropping the terms involving  $\lambda^6$  in  $\chi_2$  (that is, the terms in square brackets in equation (73)) gives slightly lower values of the ratio  $M_\alpha/M_0$ , especially for lower values of  $N$ . For example, for  $N = 3$ , the value of the ratio obtained when the terms involving  $\lambda^6$  are not included is 0.840 whereas the value is 0.865 when these terms are included. For  $N = 8$ , however, the two values are 0.957 and 0.964; thus there is almost complete convergence even when the  $\lambda^6$  terms are not included in the value of  $\chi_2$ .

## EXPERIMENTAL RESULTS AND COMPARISONS WITH THEORY

### Experimental Results

Experimental values of the apparent additional mass of a scalloped cylinder configuration, a clustered cylinder configuration, and a single circular cylinder were determined by using water as a medium. The outer boundary of a cross section of the scalloped cylinder configuration (see fig. 2) is described by equation (54) with  $N = 8$ . The outer boundary of the clustered cylinder configuration (fig. 4) is described by equation (68) with  $N = 8$ .

All the models were about 15.4 inches long and both the scalloped cylinder and clustered cylinder configurations had maximum radii of about 2.7 inches. The radius of the circular cylinder was 3.0 inches.

Each model was equipped with end plates and was suspended by 8 small cables arranged as shown in figure 6. The intended purpose of the end plates was to increase the effective length of the models and the circular cylinder model was tested to obtain an estimate of the adequacy or effectiveness of the end plates.

A cylindrical configuration suspended as indicated in figure 6 will behave as a simple pendulum with arm length  $l$  when each of the 8 cables is initially displaced through the same angle  $\beta_0$  (see view (b) in fig. 6) and released simultaneously. Hence, if the model is suspended in a fluid of density  $\rho$  and if all forces that contribute to drag and damping are neglected, the equation of motion may be expressed in terms of the angle  $\beta$  as

$$(M + \bar{M}_\alpha) l \ddot{\beta} = -gV(\rho_c - \rho)\beta \quad (76)$$

where  $M$  denotes the mass of the model (cylinder plus end plate),  $\bar{M}_\alpha$  denotes the total mass of fluid accelerated by the cylinder or the apparent additional mass,  $V$  denotes the volume of the model,  $\rho_c$  denotes the mean density of the model, and  $g$  is the acceleration due to gravity. The appropriate solution to equation (76) is  $\beta = \beta_0 \cos \omega t$  from which one can obtain the following expression for  $\bar{M}_\alpha$

$$\bar{M}_\alpha = \frac{gV(\rho_c - \rho)}{l\omega^2} - M \quad (77)$$

Thus, with a knowledge of  $g$ ,  $V$ ,  $\rho_c$ ,  $\rho$ ,  $l$ ,  $M$ , and the measured frequency  $\omega$  of the pendulum one can determine  $\bar{M}_\alpha$ . In comparing experimental results with calculated results, it was found convenient to express  $\bar{M}_\alpha$  as a fraction  $\delta$  of the maximum radius  $R_m$  of the cylinder as

$$\bar{M}_\alpha = \pi\rho(\delta R_m)^2 L \quad (78)$$

where  $L$  is the length of the configuration. Substituting this expression into equation (77) and solving for  $\delta$  gives

$$\delta = \left\{ \frac{1}{\pi \rho R_m^2 L} \left[ \frac{gV(\rho_c - \rho)}{\omega^2} - M \right] \right\}^{1/2} \quad (79)$$

### Comparisons of Experimental Results With Analytical Results

As may be determined from the preceding section or from figures 3 and 5, the calculated results correspond to a value of  $\delta$  of about 0.96 for the scalloped configuration and about 0.98 for the clustered cylinder configuration. The calculated value for the circular cylinder configuration is, of course, unity.

Values of  $\delta$  determined experimentally and analytically for the three configurations tested are given in columns 8 and 9, respectively, of table I. The difference between the analytical and experimental values of  $\delta$  for the circular cylinder (1.00 and 0.975) were used as a measure of the error in the experiment which was due to such things as the neglect of drag forces on both the configurations and the suspension cables, effect of wave motion, and possibly other factors in the equation of motion. Hence, the experimentally determined values of  $\delta$  for the scalloped cylinder configuration (0.938) and the clustered cylinder configuration (0.941) were multiplied by the ratio  $\delta_{\text{anal}}/\delta_{\text{exp}}$  of the circular cylinder to obtain the adjusted experimental values which are presented in column 10 of table I. Comparison of the analytical and experimental values of  $\delta$  shows that the values obtained by analysis are a bit high but still in substantial agreement with measured values.

### CONCLUDING REMARKS

It is concluded from the foregoing analysis and experimental evidence that the apparent additional mass of scalloped and/or clustered cylinder configurations can be accurately estimated from a knowledge of the cross-sectional area and the first few coefficients of a Fourier expansion of the logarithm of the radius vector of the configuration. It is remarked that the analytical procedure employed is not restricted to configurations for which equations of the periphery are known analytically because, with the use of harmonic analyses, the procedure can be readily adapted to graphically given configurations.

Langley Research Center,  
National Aeronautics and Space Administration,  
Langley Station, Hampton, Va., May 14, 1962.

## REFERENCES

1. Lamb, Horace: Hydrodynamics. Sixth ed., Dover Publications, 1945, p. 66 and following.
2. Milne-Thompson, L. M.: Theoretical Hydrodynamics. Second ed., The Macmillan Co., 1950, pp. 234-235.
3. Munk, Max M.: The Aerodynamic Forces on Airship Hulls. NACA Rep. 184, 1924.
4. Jones, Robert T.: Properties of Low-Aspect-Ratio Pointed Wings at Speeds Below and Above the Speed of Sound. NACA Rep. 835, 1946.
5. Bryson, Arthur E., Jr.: Stability Derivatives for a Slender Missile With Application to a Wing-Body-Vertical-Tail Configuration. Jour. Aero. Sci., vol. 20, no. 5, May 1953, pp. 297-308.
6. Nielsen, Jack N.: Missile Aerodynamics. McGraw-Hill Book Co., Inc., 1960.
7. Ashley, Holt, and Asher, Gifford W.: On the Virtual Mass of Clustered Boosters. Rep. No. 60-7, Fluid Dynamics Res. Lab., M.I.T., and Aero-Space Div., Boeing Airplane Co., Dec. 1960.
8. Theodorsen, T., and Garrick, I. E.: General Potential Theory of Arbitrary Wing Sections. NACA Rep. 452, 1933.
9. Garrick, I. E.: Conformal Mapping in Aerodynamics, With Emphasis on the Method of Successive Conjugates. Construction and Applications of Conformal Maps, Appl. Math. Series 18, National Bur. Standards, Dec. 26, 1952, pp. 137-147.
10. Robinson, A., and Laurmann, J. A.: Wing Theory. Cambridge Univ. Press, 1956.
11. Tricomi, F. G.: Integral Equations. Interscience Publ. Inc. (New York), 1957.
12. De Haan, D. Bierens: Nouvelles tables d'intégrales définies: G. E. Stechert & Co. (New York), 1939, p. 474, table No. 334.
13. Whittaker, E. T., and Watson, G. N.: A Course of Modern Analysis, Fourth ed., Cambridge Univ. Press, 1958.

TABLE I.- TABLE OF PERTINENT DATA FOR CONFIGURATIONS CONSIDERED, SHOWING  
COMPARISONS BETWEEN MEASURED AND CALCULATED VALUES OF  $\delta$

Type of cylinder	$\rho$ , slugs/cu ft	$R_m$ , in.	$L$ , in.	$l$ , in.	$\omega$ , radians/sec	$gV(\rho_c - \rho)$ , lb	$M$ , lb-sec <sup>2</sup> /ft	$\delta$		
								From measurements	From analysis	Adjusted experimental values
Scalloped	1.932	2.706	15.42	36.625	2.287	24.125	1.163	0.938	0.964	0.962
Clustered	1.932	2.706	15.42	36.625	2.283	23.75	1.141	.941	.982	.965
Circular	1.932	3.000	15.72	36.00	2.232	29.00	1.452	.975	1.00	1.00

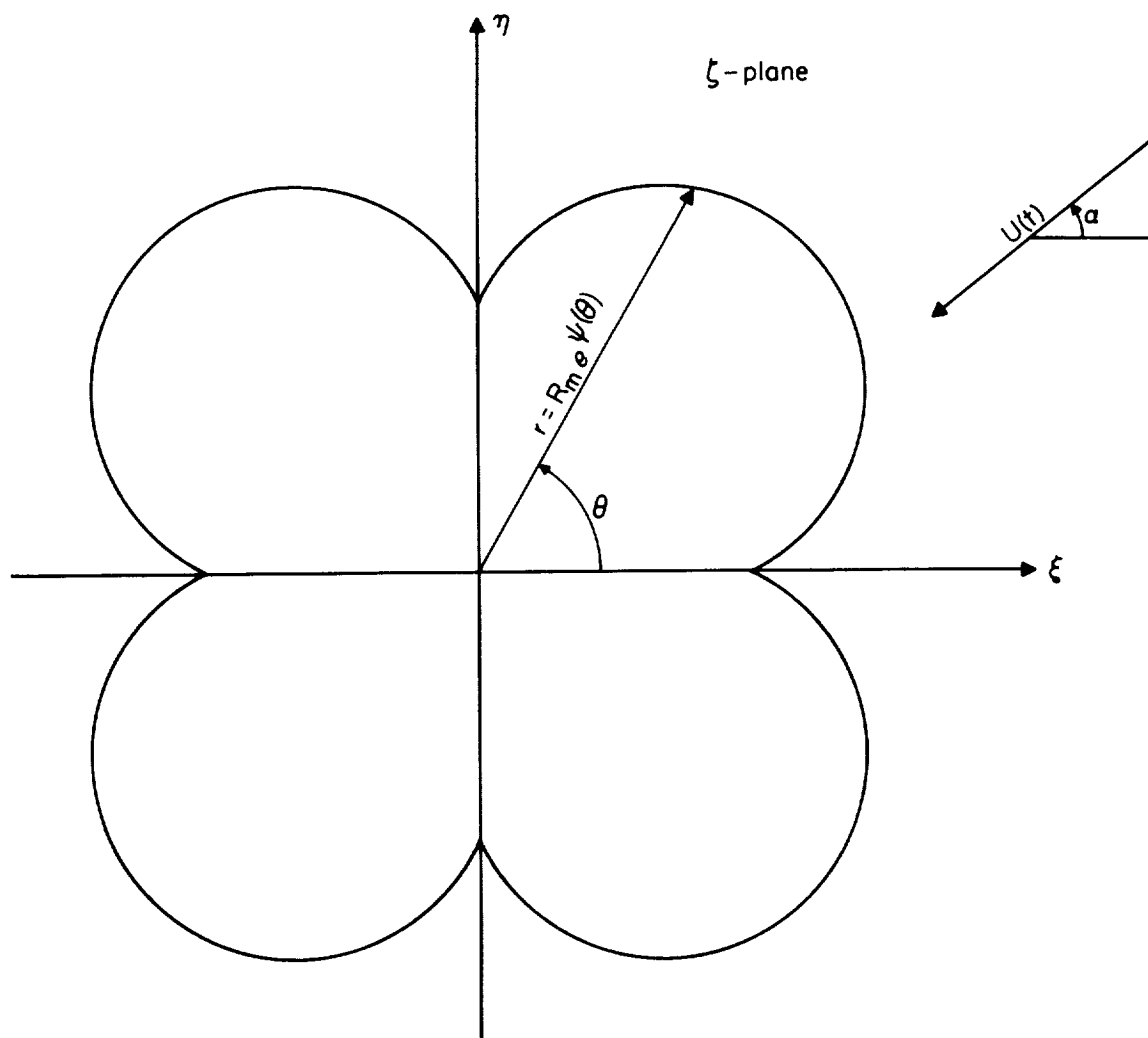


Figure 1.- Rectangular and polar coordinate systems for a clustered and/or scalloped cylinder configuration in the  $\zeta$ -plane.  $N = 4$ .

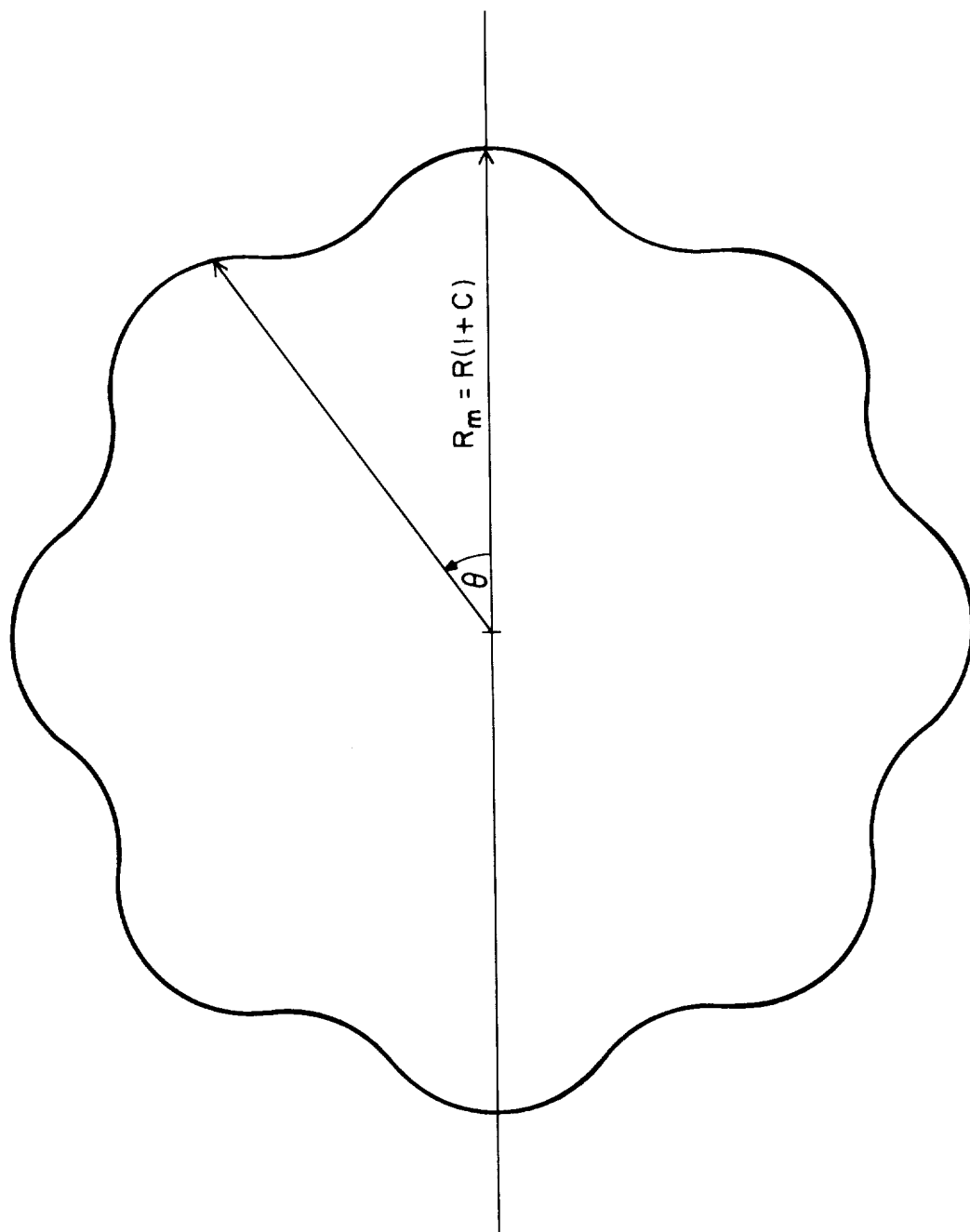


Figure 2.- Scalloped configuration considered.  $N = 8$ .

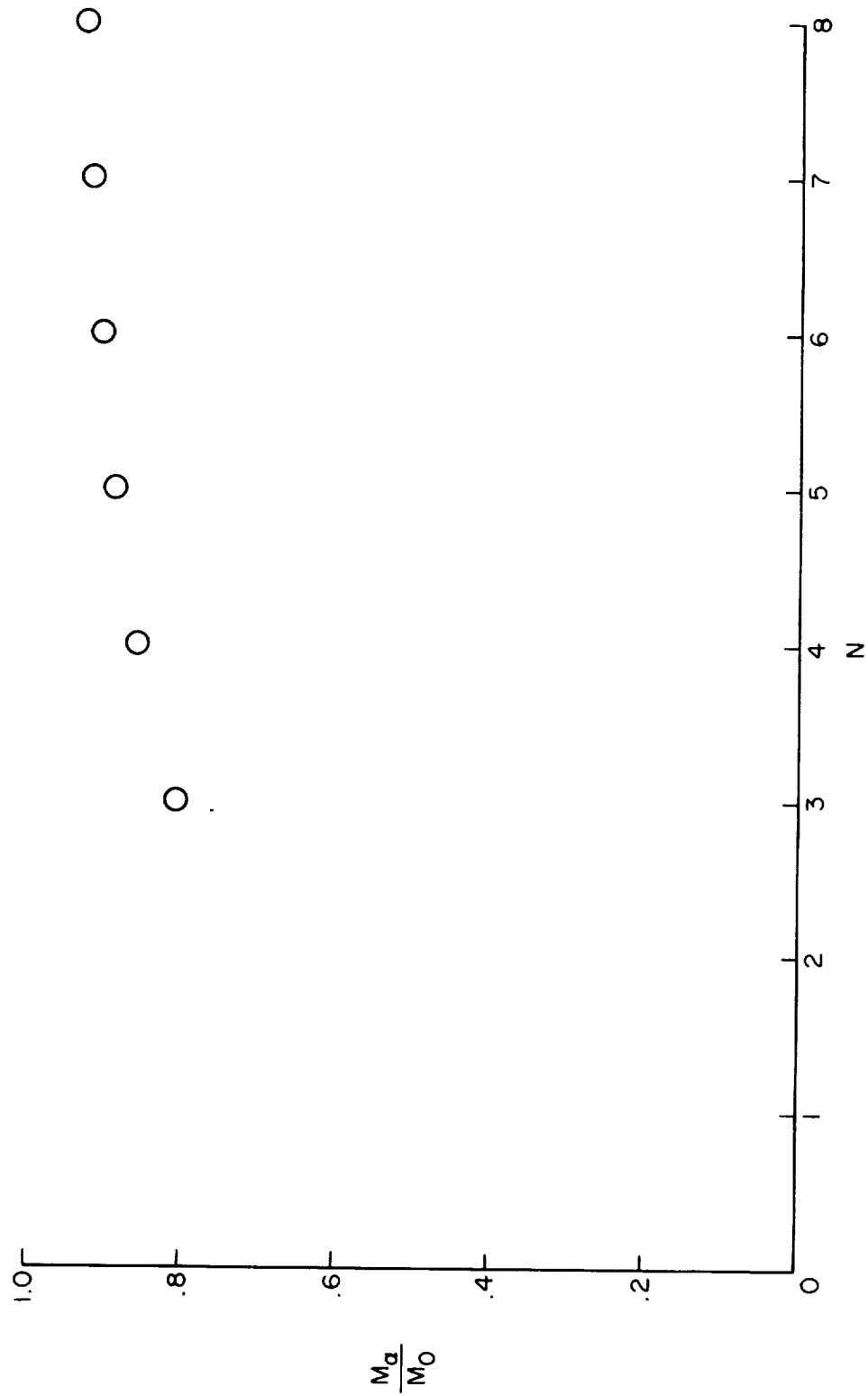


Figure 3.- Ratio of apparent additional masses for scalloped configurations considered.



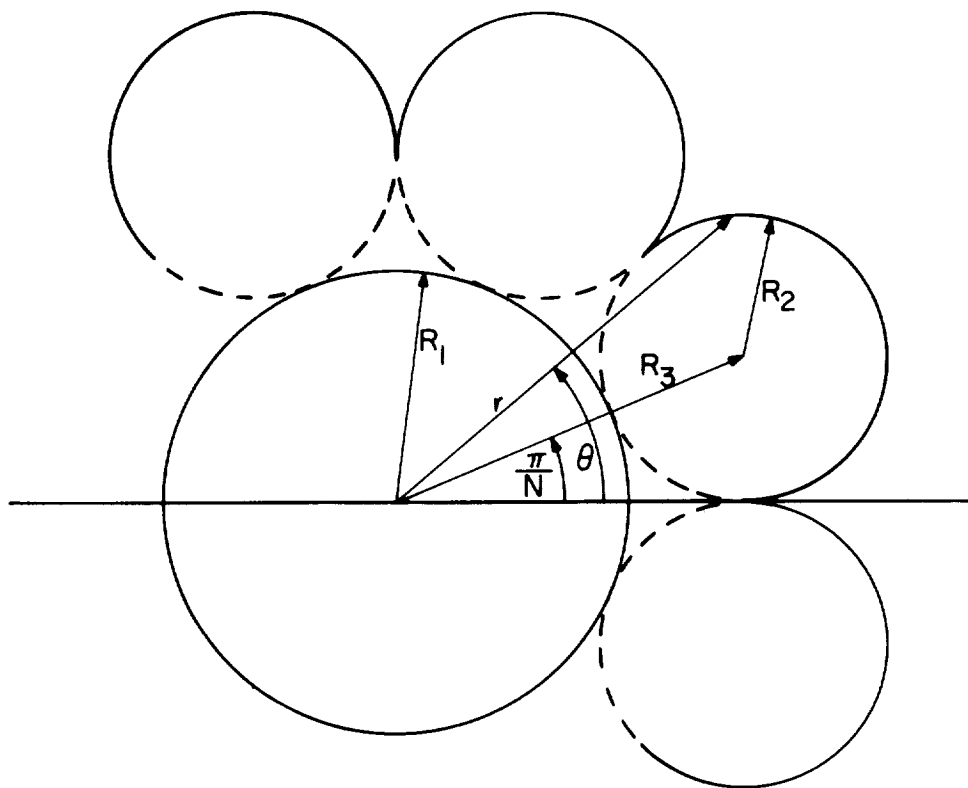


Figure 4.- Clustered cylinder configuration with  $N = 8$ .

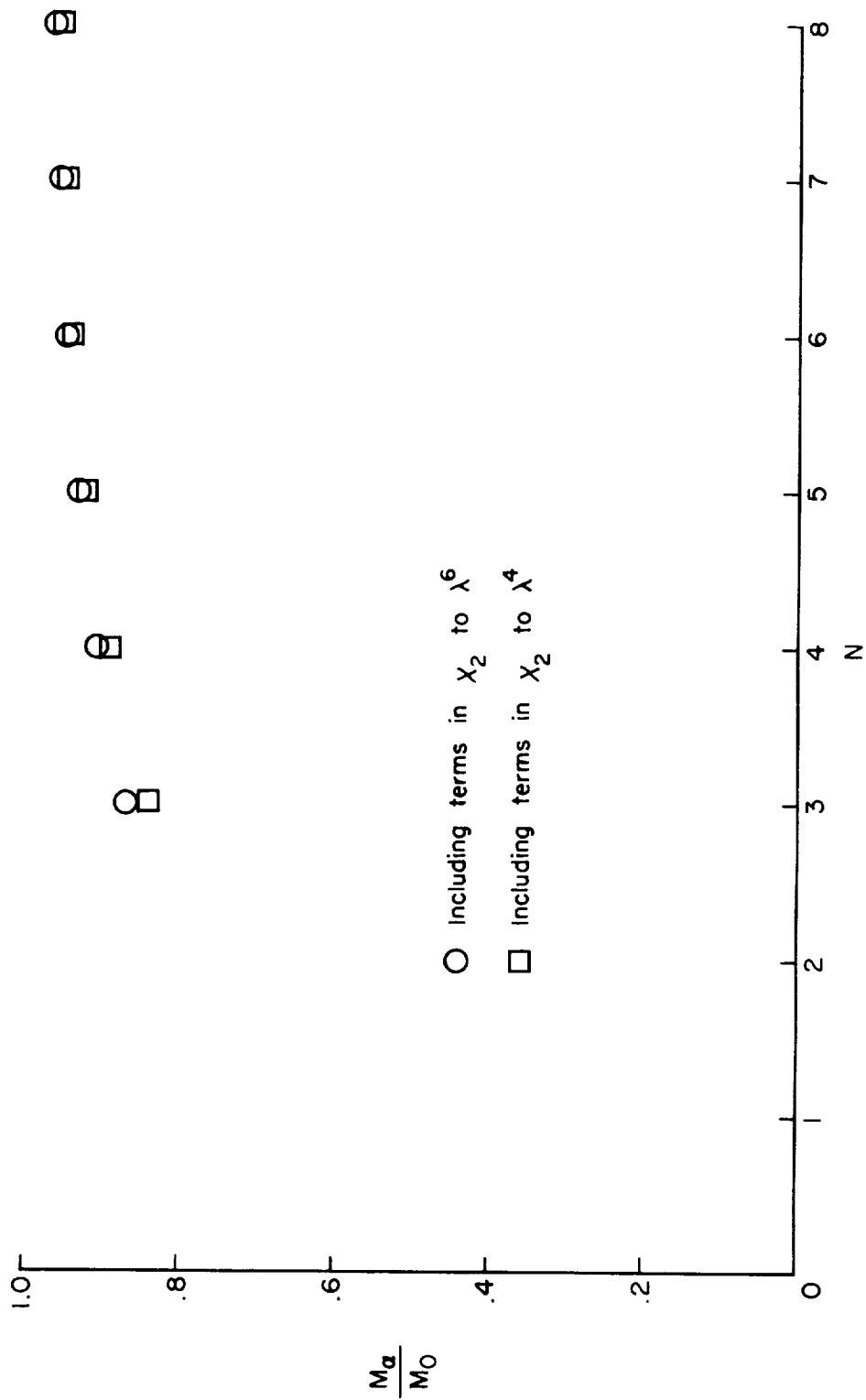
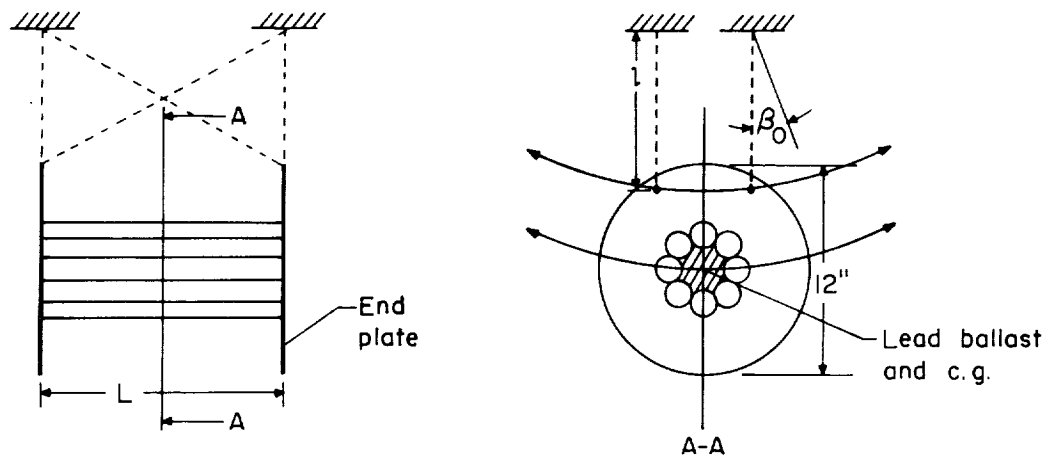


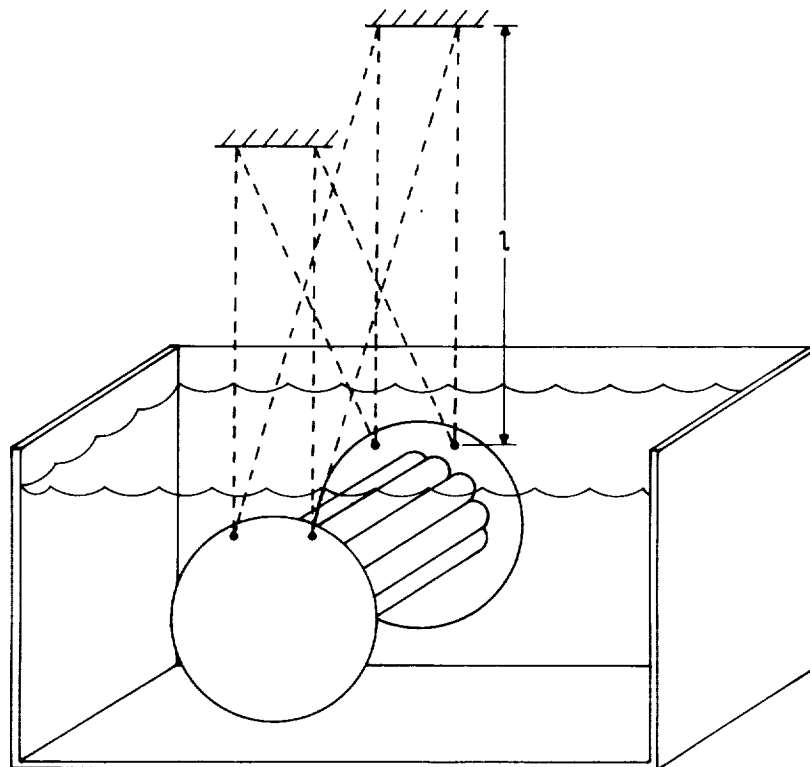
Figure 5.- Ratio of apparent additional masses for clustered cylinder configuration.





(a) Side view of suspended cylinder.

(b) End view of suspended cylinder.



(c) Cutaway view of setup.

Figure 6.- Sketch of experimental setup showing the clustered cylinder configuration with  $N = 8$  and the suspension system.



